Sensors & Transducers, Vol. 150, Issue 3, March 2013, pp. 97-105

Sensors & Transducers

http://www.sensorsportal.com

Simulation Study of Bubble Detection Using Dual-Mode Electrical Resistance and Ultrasonic Transmission Tomography for Two-Phase Liquid and Gas

Fazlul Rahman MOHD YUNUS, Noor Azida NOOR AZLAN, Nor Muzakkir NOR AYOB, Muhammad Jaysuman PUSPPANATHAN, Mohd Fahajumi JUMAAH, C. L Goh, Ruzairi ABDUL RAHIM, Anita AHMAD, Yusri Md YUNUS, Herlina ABDUL RAHIM

Process Tomography and Instrumentation Research Group (PROTOM-i), INFOCOMM Research Alliance, Faculty of Electrical Engineering, Universiti Teknologi Malaysia
81310 UTM Skudai, Johor, Malaysia
Tel.: +607-5537801, fax: +607-5537811
E-Mail: ruzairi@fke.utm.my, frahman3@live.utm.my

Received: 12 February 2013 /Accepted: 19 March 2013 /Published: 29 March 2013

Abstract: Tomography is a process of imaging parameters in industrial applications. It can be based on different sensing methods; ultrasound and electrical impedance sensing methods are both sensitive to the particular characteristics of a material. These imaging methods have been shown to be practical instruments for process monitoring in the process industry. However the achieved image can be low in quality and restricted in resolution due to ill-posedness of the inverse problems and limited data. To further enhance the spectral images, this paper proposed combination of ultrasound transmission tomography (UTT) and electrical resistance tomography (ERT) to monitor a static two-phase liquid and gas. This paper presents the modeling approach for three dimensional (3D) geometries with linear finite element method (FEM) using COMSOL multiphysics. The modeling approach is aimed to determine the ability of dual-modality system in detecting bubbles with different sizes located at the center medium in acrylic vessel. Simulation results showed that the dual-modality system has the potential and can be implemented as alternative technique to visualize bubble with minimum radius of 5 mm located at center of the acrylic vessel. *Copyright © 2013 IFSA.*

Keywords: Electrical resistance tomography, Ultrasonic tomography, Opposite excitation, Acoustics impedance, Time-of flight, Bubble.

---

1. Introduction

In Tomography systems, the physical properties of a material distribution can be described by either permittivity or conductivity properties. A tomogram image of the phase interactions is important to understand the operation of multi-phase flows. The image is provided by different measurement techniques with quantitative local and global dynamic information of the flow that is useful for system design and control [1]. Single modality tomography systems such as electrical capacitance tomography (ECT), electrical impedance tomography (EIT), electrical resistance tomography (ERT) have been extensively and successfully implemented in industrial process for several decades. Although single modality tomography offers simplicity, low-cost, no-radiation, robust, non-intrusive and capable to provide sufficient information for some applications, however in more complex application such as three-phase flow process more information is required [2]. Complex process requires multiple measurements to quantify each of the medium individually. In recent years some multi-modality tomography systems have been developed for multi-phase flow [3-7]. Many application of multi-modality tomography have been found in monitoring for industrial process such as hydrocarbon flow measurement and material classification.

Multimodality tomographic system is defined as one in which two or more different sensing modalities are used to locate or measure different constituents in the object space [8]. These systems provide component specificity by using independent component sensing in the measurement volume, by electrical properties such as capacitance and gamma-ray sensing in oil/water/gas tomography. In single modality tomography system, ERT is used to visualize conductivity distribution of medium to be imaged and ultrasonic transmission tomography (UTT) is used to distinguish medium boundaries based upon interactions between the incident ultrasonic waves and objects to be imaged [9]**.** UTT has the benefit of detecting edges accurately, while it is not possible to reconstruct permittivity values of the involved materials. In contrast ERT with nonlinear iterative reconstruction enables the quantification in terms of absolute conductivity values. However, due to needful of regularization, no sharp edges can be resolved. Because of the complementary properties form this modalities, it is possible to combine the ERT and UTT to produce dual-modality tomography sensor. With the proposed system the ERT can be used to visualize the conductive component and UTT can be used to visualize the boundaries medium of interest.

2. System Overview

Multi-modal systems inherently encourage a systematic approach in contrast to current generation process tomography systems that are complex, expensive and designed primarily for the prototype laboratory. A successful system must allow individual sensor data to be collected and combined effectively. It must therefore exploit opportunities for rationalization and sharing of resources, and deal with hazards of mutual interference [10]. The proposed system is based on the use of two types of sensing elements which consists of 16 electrodes of ERT and 16 ultrasonic transceivers located internally and externally respectively in a axial distance around the circumference of an acrylic pipe which are shown in Fig. 1.

For electrical resistance tomography (ERT), opposite excitation is applied to the electrodes and the resulting changing in voltages is measured. This method is sensitive to conductivity change (as in adjacent strategy) as current flows through the center point of the cross-section. This gives rise to even distribution of currents, leading to good image characterization**.** Based on current-voltage relationship the electrical properties of the conductivity distribution can be reconstructed. In the ERT system, the effective spatial resolution of the reconstructed images depends upon the number of elements in the FEM. Greater number of elements, the better the resolution. The number of independent measurements, depends upon the number of electrodes, N, should also be increased. In the adjacent measurement mode, the number of independent measurements (L) is given by the following equation:

$$L = \frac{N(N-3)}{2}, \quad (1)$$

where N is the number of electrodes. Form equation (1), for the 16 electrodes a total of 104 independent measurements can be obtained.

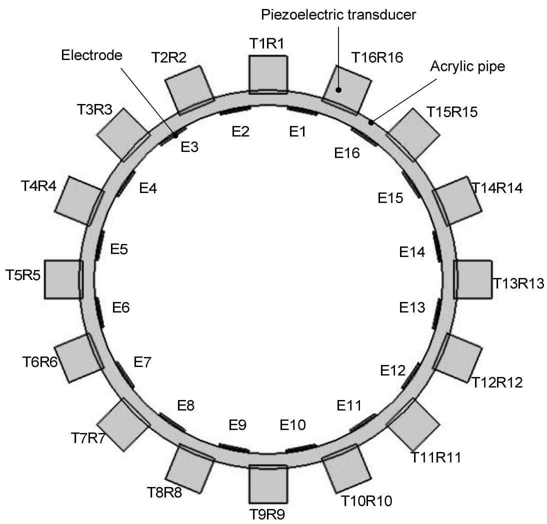

Fig. 1. Cross section of the dual-modality ERT/UTT tomography system

Similar to the ERT electrodes, the 16 piezoelectric (PZT) ultrasonic transceivers are located externally around the circumference of the pipeline. By using the transmission mode and fan shaped beam projection technique 16 transceivers with beam angle of 125^0 were located side by side non-invasively along the periphery of the pipeline. From Fig. 2, it is shown only 9 transceivers are located within the beam coverage at each projection. For full scan a total of 16 observations will be made with 9 received channels per observation hence 144 independent measurements can be obtained. Ultrasonic with dual function (transmitter and receiver) or transceivers is implemented because of its advantages to produce same quality images compared to the individually transmitter-receiver system. Therefore the transducer can only be a transmitter or receiver at any one time. The accurate timing for the system is crucial since small timing errors could lead to erroneous of measurement data [11].

The proposed system will implement the transmission mode as the measurement strategy. The transmission mode is the measurement of the changed of properties of the transmitted acoustics wave. The properties are sensitive by the material of medium in the measuring volume. The changes of physical properties can be the intensity and transmission time or time-of flight (tof) [12].

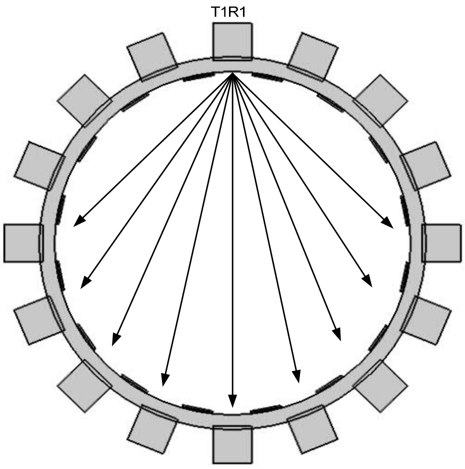

Fig. 2. Single scanning geometry using fan shaped of 125^0 beam projection

3. Ultrasonic Transmission Tomography

Ultrasonic sensors have been successfully applied in process particularly in flow measurement. Ultrasonic sensors systems are based upon interactions between the incident ultrasonic waves and object to be imaged. It is applicable only to process where a significant interaction occurs [7]. Previous research had been carried out in multiphase flow measurements that give promising results using the ultrasonic sensors [13]. The interaction of ultrasonic wave with a material can be represented with its acoustics impedance which can be described as:

$$Z = \rho c \, , \tag{2}$$

where

c = the velocity of sound (m/s);

Z = the acoustics impedance (kg/m^{2}s);

ρ = the medium density (kg/m^3).

The velocity of ultrasonic wave is determined principally by the compressibility of propagating medium. A medium with high compressibility for example air caused slow ultrasound velocity, in contrast a medium with low compressibility for example liquid, yields fast propagation speed. In this paper the physical model parameters and ultrasonic properties of selected materials for simulation purposes are shown in Table 1 and Table 2 respectively.

Table 1. Physical parameters and dimension.

No.	Item	Value
1.	Number of electrodes	16
2.	Electrode size	12 mm × 90 mm
3.	Inner diameter pipe	94 mm
4.	Outer diameter pipe	100 mm
5.	Drive current	1 mA, 100 kHz

Table 2. Material properties of ultrasonic application.

No.	Material	Velocity (m/sec)	Acoustics impedance (kg/m^{2}s)	Density (kg/m^{2}s)
1.	Acrylic plastic	2,680	3.08	1,160
2.	Sea water	1,550	1.55	1,029
3.	Air	331	409.4	1,183
4.	Aluminum	6,420	18.1	2,700

Process tomography using ultrasonic sensing relies upon detectable interactions both in a homogeneous transmission medium and from interfaces, for example gas bubbles in a liquid. In process application with variety of intersection occur caused attenuation to incident waves due to the presence of object or field between receivers and transmitters. It is understood that the greater the difference in impedance at the interface the greater the amount of energy will be reflected [14]. The reflection of diffraction (P_r) and transmission coefficient (P_t) can be defined as:

$$P_r = \left(\frac{P_r}{P_t}\right)^2 = \left(\frac{(Z_2 - Z_1)}{(Z_2 + Z_1)}\right)^2 \tag{3}$$

$$P_t = \left(\frac{P_t}{P_i}\right)^2 = \left(\frac{2Z_2}{(Z_2 + Z_1)}\right)^2 \tag{4}$$

The given properties thus complement with other imaging technologies such as ECT and EIT [11]. The fan beam has been chosen because of the cover area with 125^0 is bigger for the receiver to received signal transmitted by the transmitter [13]. The ultrasonic wave has found to have several specific problems which may limit its application. The speed of sound in gas limits the data acquisition rate and particle impact on the flow pipe may produce very high levels of noise at the transducer [11].

In transmission mode method it emphasizing the amplitude received by the receiver and the arrival time analysis. This analysis is based on the properties that finite time is required for an ultrasonic disturbance to move from one location inside the pipe. The observation time (t_s) is the first peak to arrive after the time-of-flight corresponds to a straight path. This is shown in Fig. 3. By applying sampling amplitude for every receiving sensor the information given by transmission mode method can be obtained.

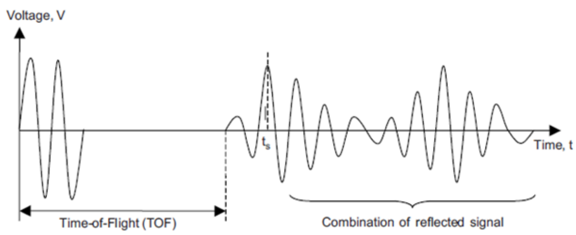

Fig. 3. Transmitter and receiver signal.

In this paper, simulation was performed using piezoelectric transducer (PZT) with resonance frequency at 315kHz. Ultrasonic transducer with high frequency is implemented because of to increase the sensitivity of the system and to increase the ability in detecting small discontinuity in the medium for example air bubble. However selecting high frequency transducer would decrease the penetration depth. As general rule the discontinuity must be larger than one-half of the wavelength for the discontinuity to be detected by the system. The relationship between wavelength and frequency and velocity is given by equation below:

$$\lambda = \frac{c}{f} \tag{5}$$

where

λ = ultrasonic beam wavelength;

c = speed of sound;

f = ultrasonic frequency.

4. Electrical Resistance Tomography

Electrical resistance tomography (ERT) is a particular case of electrical impedance tomography (EIT). ERT is most widely and easily implemented for purely resistive medium [15]. ERT is based on the principles that different medium have different electrical properties. In ERT an electrical current is injected through a set of electrodes placed in a boundary of the domain of interest therefore resulting in an electrical field that is conditional by the conductivity distribution within the domain. The resulting electrical potential at the domain parameter can be measured using the remaining electrodes. For complete measurements or known as 1 scan is obtain when all electrodes are used for injection and differential potentials between all remaining pairs of adjacent electrodes are measured.

$$\nabla \bullet (\sigma \nabla \phi) = 0\,,\ \bar{r} \in \Omega \tag{6}$$

Electrodes, which are used to probe the object, function as electrodes. Current is passes between the two electrodes and produce current patterns. At the same time other electrode serves as a measurement of the electrode potential difference with respect to the ground electrode. They are used to measure the voltage drop with a reference to the sink electrode. For the following boundary conditions the integral of current density across the electrode surface is equal to the current flow.

$$\int_{e_k} \sigma \frac{\partial u}{\partial \vec{n}} dS = I_k\,,\ k = 1,2,3...K \tag{7}$$

For the part of object's surface under the current excitation electrodes the flows of current density has the form of:

$$\sigma \frac{\partial u}{\partial \vec{n}} = \vec{j} \tag{8}$$

For other surface of detection electrodes

$$\sigma \frac{\partial u}{\partial \vec{n}} = 0 \tag{9}$$

Potential value, measured at the electrode is the sum of the potential on the surface under the electrode and the voltage drop on the contact resistance of the electrode:

$$u + Z_k \sigma \frac{\partial u}{\partial \bar{n}} = U_k\,; k = 1,2,3...K \,, \tag{10}$$

where

ϕ = electric potential in the body;

σ = conductivity;

Z_k =contact impedance at k-th electrode;

U = potential at k-th electrode.

5. Simulation Results

Three types of common current excitation strategy were considered and only one excitation will be implemented into the system: (a) adjacent, (b) opposite, and (c) diagonal. Each strategy was simulated using sea water as the medium inside of acrylic vessel. Three dimensional images of the each excitation were simulated and analyzed using COMSOL.

As can be seen from Fig. 4, the field distribution of opposite excitation strategy is evenly distributed along the symmetrical lines between sources (red color) and sink (blue color) electrodes. From observation the density of current distribution in opposite excitation is higher particularly along the center pipeline. Thus, this gives better sensitivity compared with adjacent and diagonal strategy. A comparison of electrical displacement was also carried out between the excitation strategies. From Fig. 5(a), the electrical displacement of opposite strategy increased towards the center medium in homogeneous medium. A bubble of 10mm is positioned at the center pipeline and it is found that opposite excitation gives better sensitivity as shown in Fig. 5(b).

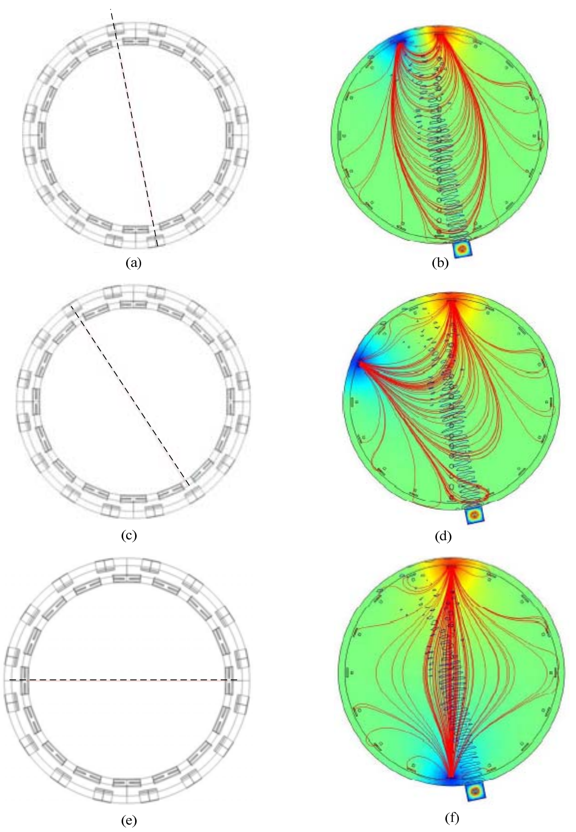

Fig. 4. Current density distribution of most three common current excitation strategy; (a)-(b) adjacent, (b)-(c) diagonal, and (d)-(e) opposite.

Fig. 6(a) shows the potential change $\Delta V / V_H$ with respect to the corresponding potential in homogeneous medium with low and high conductivity bubble at the center, near source, near sink and side position as shown in Fig. 6(a). From the simulation result, the response signal for 1mm center bubble in Fig. 7(a) is less sensitive compared with bubble with radius of 5 mm and 10 mm at the center medium. It is also observed that the 5 mm and 10 mm bubble shows similar characteristics at electrode 2, 3, 4 and 5 suggesting high current density near these electrodes. Positive potential difference occurred at electrodes 5, 6, 7 and 8 as the current density is less near these electrodes. Potential difference for 1mm bubble approximately similar with homogeneous medium shows that it is hardly to be recognized. From the simulation results, the location of bubble inside medium can caused higher potential difference near electrodes as more current are concentrated nearby. The greater the bubble size the higher difference potentials among the electrodes and the difference is more significant when the bubble is located at the boundary. It is observed by simulation that ERT has the ability to improve in sensing bubble at the center medium. However small surface potential captured by the boundary electrodes because of low excitation current, it is recommended to inject higher excitation current to achieve a good result.

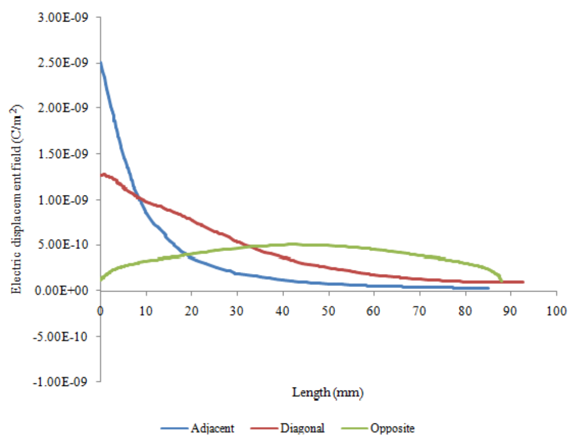

(a)

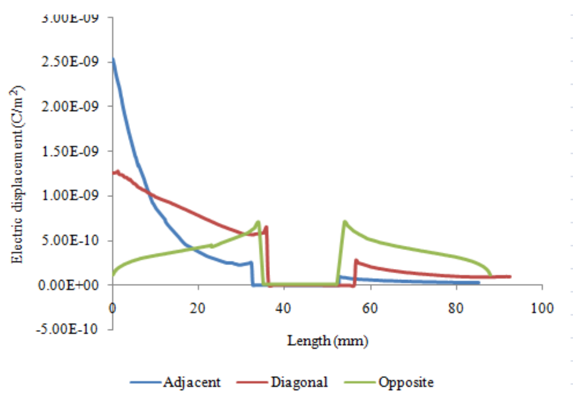

(b)

Fig. 5. Electrical displacement field of adjacent, diagonal and opposite excitation; (a) homogeneous medium, and (b) 10 mm air bubble.

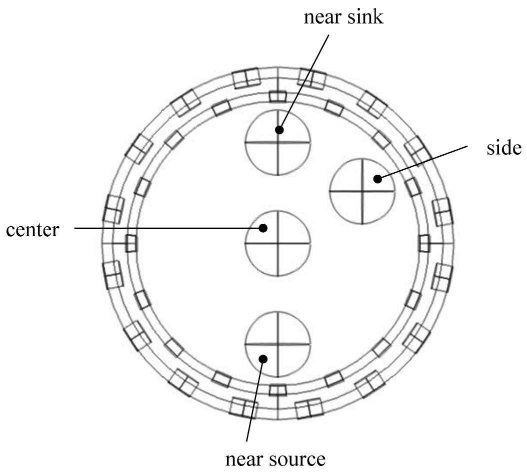

Fig. 6. Bubble at four different locations.

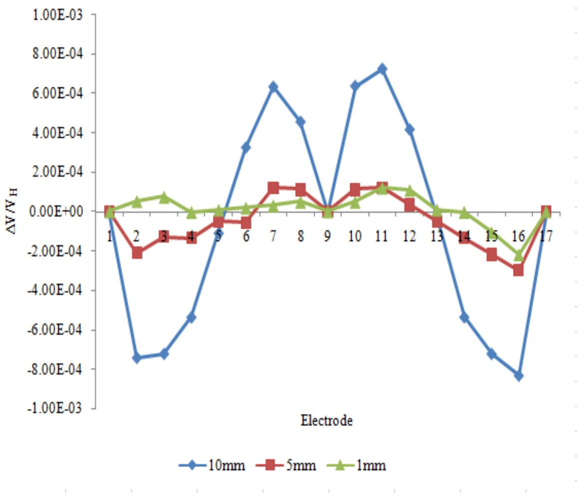

(a)

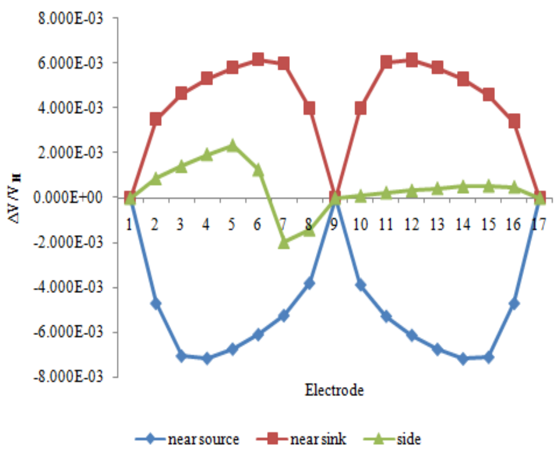

(b)

Fig. 7. Potential difference with 5mm bubble; (a) Different conductivity bubble at center pipeline, (b) Side, near sink and near source position.

Three dimensional (3D) images shown in Fig. 8. The observation can be summarized as follows:

a) In the location of two excitation electrodes the electrical displacement field is approximately zero. However the electrical displacement increased as it enters towards to the center medium.
b) The distribution of electrical displacement is obviously in non uniform field. Opposite excitation produces significant displacement with bubble at the center medium. Therefore the position and size of the bubble can be obtained according to the electrical displacement and suitable algorithm.

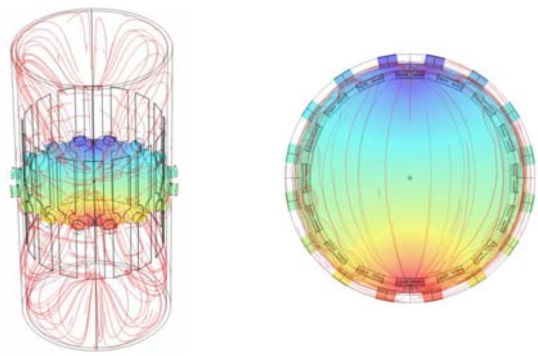

(a) (b)

Fig. 8. Three-dimensional (3D) simulation of dual-modality with 1mm center bubble using opposite strategy.

In ultrasonic tomography system, greater distinct of acoustics impedance will results greater energy to be reflected. In contrast, if the material impedance similar with the medium inside the vessel most of the energy will be transmitted. To verify this, a simulation was carried out using piezoelectric transducer (PZT) with resonance frequency 315 kHz. Using the same model a pulse signal is applied to T_1R_1 at frequency 315 kHz. The time-of flight and the attenuation signal is measured at T_9R_9 according to different bubble sizes located at the center medium. From Table 2, because the speed of sound in air and water is highly distinct, the time of flight of the received signal in homogeneous is faster compared when air bubble is located at the center medium. The received signal has decreased due some of transmitted wave has been reflected by bubble during the propagation. The simulated time-of flight of homogeneous and 1mm bubble is illustrated in Fig. 9.

Table 2. Time-of flight (tof) simulation values for transceivers T_9R_9.

T_xR_x	Bubble diameter (mm)	Time-of flight(μs)	Peak acoustics pressure (Pa)
T_9R_9	0 mm	36.0	0.935
	1 mm	36.5	0.792

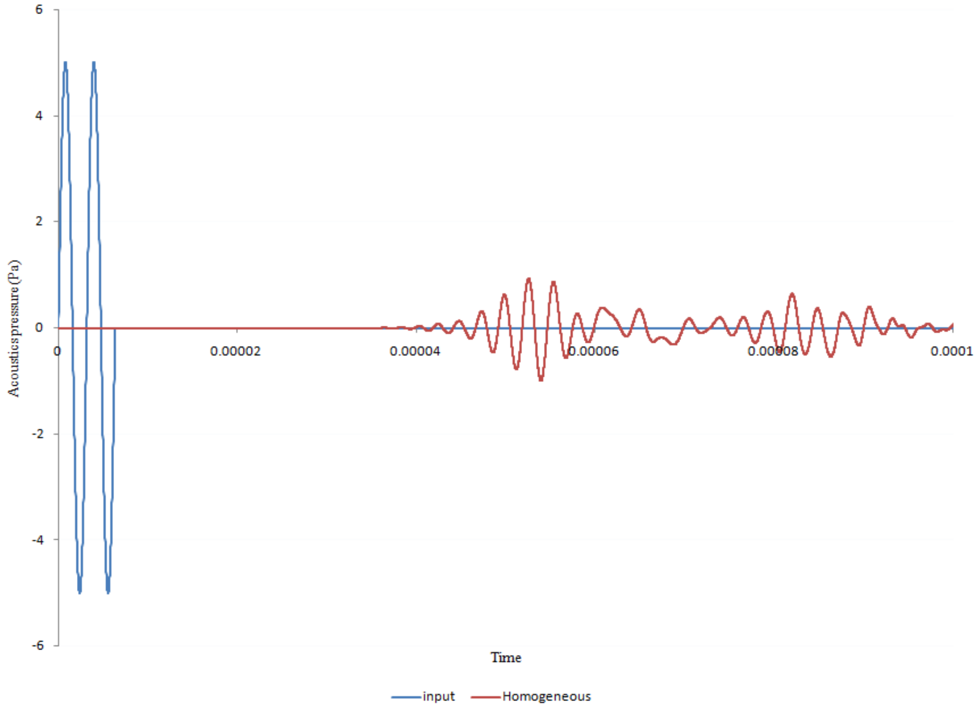

(a)

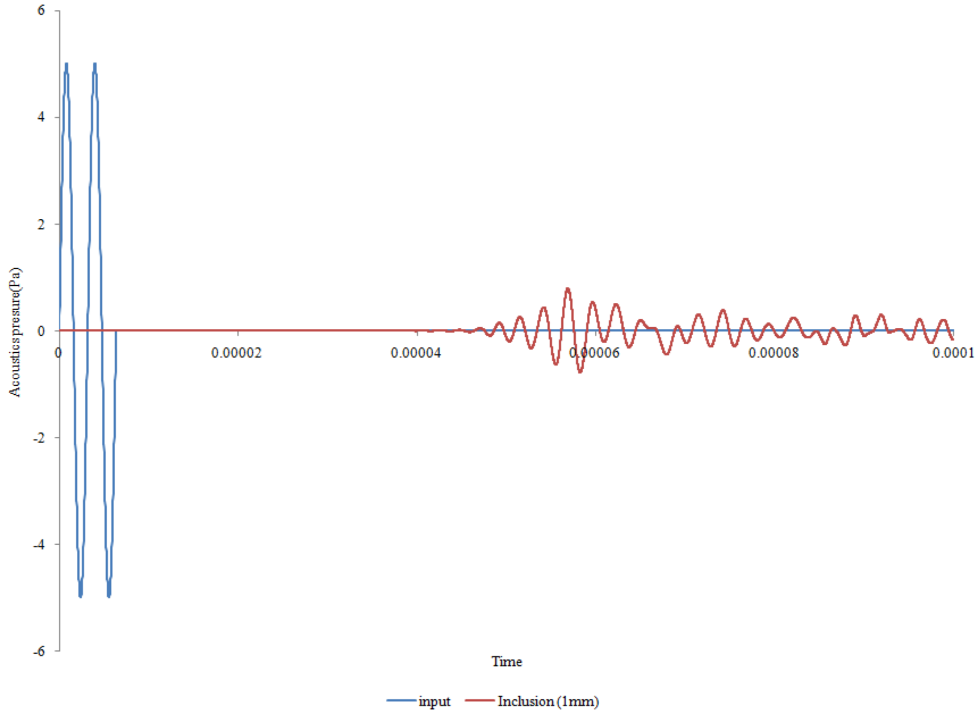

(b)

Fig. 9. Signal received at transceiver T_9R_9; (a) homogeneous medium, (b) 1 mm bubble.

From Table 3 below, it is estimated that 86.33 % of transmitted ultrasonic wave is capable to penetrate the acrylic/liquid interface. The transmitted will be received by the transceivers and then amplified to appropriate value before measurements are to be taken. Large distinct acoustics impedance between liquid/gas interfaces caused 98.50 % of the ultrasonic wave is reflected and only 1.5 % will be received by transceiver at T_9R_9. This clearly indicates that transmitted ultrasonic wave is detectable at T_9R_9 with maximum bubble of 1mm along the transmission path as illustrated in Fig. 10. In contrast bubble greater than 1mm will fully blocked the transmitted wave form being received by the receiver.

Table 3. Ultrasonic propagation properties in homogeneous medium.

Interaction	Reflection coefficient (%)	Transmission coefficient (%)
Acrylic/ liquid	13.67	86.33
Liquid/gas	98.50	1.50

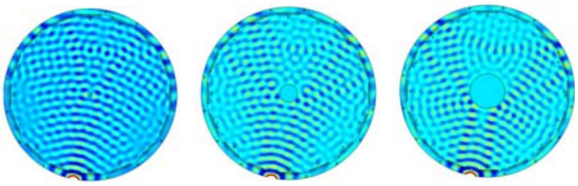

(a) (b) (c)

Fig. 10. Acoustics pressure field with different air bubble; (a) 1 mm, (b) 5 mm, and (c) 10 mm.

6. Discussion

From the simulation result it is possible to combine electrical resistance and ultrasonic transmission tomography at the same plane to improve the reconstruction images particularly at the center medium. From the simulations that were carried out it are obviously shows the ability of ERT to determine bubble at the center medium. Although the displacement values obtained was very small, it can be improved by applying more intense current excitation at high frequencies. Optimum range of the measuring signal frequency with respect to the measurement accuracy must carry according to the frequency characteristics [16].

In ultrasonic transmission numerical methods proved that almost no energy wave was received at the opposite transceiver with center bubble with radius greater than 5 mm along the transmission path. Therefore large bubble can be identified and observed. Further improvements in measurement resolution using dynamic algorithm instead of static algorithm is essentially required to resolve this problem.

7. Conclusion

In this paper, dual-modality tomography system has been proposed by combining the soft-field and hard-field technique to improve sensitivity of bubble at the center medium in acrylic vessel. In the proposed system, the conductivity distribution can be developed by using the surface potential from the 16 electrodes and similarly to the ultrasonic image can be reconstructing by using the time-of flight from the ultrasonic wave interaction. The next process will focused on development of reconstructed images of conductivity and ultrasonic properties from measurement and simulation data.

Acknowledgements

The authors would like to thank the Faculty of Electrical Engineering, Universiti Teknologi Malaysia and Process Tomography and Instrumentation Research Group (PROTOM-i) for valuable discussions and constructive comments that have been useful during preparation of this paper.

References

[1]. Wang, F., et al., Electrical Capacitance Volume Tomography: Design and Applications, *Sensors*, 2010, 10, 3, pp. 1890-1917.

[2]. C. Qiu, B. S. Hoyle, and F. J. W. Podd, Engineering and application of a dual-modality process tomography system, *Flow Measurement and Instrumentation*, 18, 5-6, 2007, pp. 247-254.

[3]. Ziqiang Cui, et al., An Integrated ECT/ERT Dual Modality Sensor, in in *Proceedings of the IEEE International Instrumentation and Measurement Technology Conference*, Singapore, 2009, p. 1434-1438.

[4]. Baoliang Wang, Zhiyao Huang, and H. Li, Design of high-speed ECT and ERT system, in *Proceedings of the 6th International Symposium on Measurement Techniques for Multiphase Flows 2009, Journal of Physics: Conference Series*, 147 p. 1-8.

[5]. Tom Dyakowski, et al., A Dual Modality Tomography System for Imaging Gas/Solids Flows, *Particle & Particle System Characterization*, 23, 3-4, 2006, pp. 260-265.

[6]. Cong Xu and F. Dong, Electrical Resistance Tomography System Based on Compact PCI for Multiphase Flow Measurement, in *Proceedings of the IEEE Instrumentation and Measurement Technology Conference*, Binjiang, China, 2011, p. 1-6.

[7]. Gerald Steiner, Hannes Wegleiter, and D. Watzenig, A Dual-Mode Ultrasound and Electrical Capacitance Process Tomography Sensor, in *Proceedings of the IEEE Sensors*, Irvine, CA, 2005, p. 696 - 699.

[8]. Bjørn Tore Hjertaker, et al., Multimodality Tomography for Multiphase Hydrocarbon Flow Measurements, *IEEE Sensors Journal*, 5, 2, 2005, pp. 153-160.

[9]. Williams, R. A. and M. S. Beck, Process Tomography: Principles, techniques and applications, *Butterworth Heinemann Ltd.*, 1995, p. 580.

[10]. B. S. Hoyle, et al., Design and application of a multi-modal process tomography system, *Measurement and Science Technology*, 12, 8, 2001, pp. 1157-1166.

[11]. M. H. Fazalul Rahiman, Z. Zakaria, and R. Abdul Rahim, Ultrasonic Process Tomographic Imaging Sensor: An Approach Utilising Transceivers Method. in *Proceedings of the IEEE International Conference on Computer and Communication Engineering*, Kuala Lumpur, 2008.

[12]. Mohd Hafiz Fazalul Rahiman, Ruzairi Abdul Rahim, and N. M. N. Ayob, The Front-End Hardware Design Issue in Ultrasonic Tomography, *IEEE Sensors Journal*, 10, 7, 2010, pp. 1276-1281.

[13]. Y. Abdul Wahab, et al., Application of Transmission-Mode Ultrasonic Tomography to Identify Multiphase Flow Regime, in *IEEE Proceedings of the International Conference on Electrical, Control and Computer Engineering*. Pahang, Malaysia, 2011, pp. 119-123.

[14]. Hoyle, B. S., Process Tomography using ultrasonic sensors, *Measurement and Science Technology*, 7, 3, 1996, pp. 272-280.

[15]. M. G. Rasteiro, et al., Electrical Tomography: a review of Configurations and Applications to Particulate Processes, *KONA Powder and Particle Journal*, 29, 2011, pp. 67-80.

[16]. Ping, W., et al., Study on sweeping frequency of electrical impedance tomography system, in *World Automation Congress, WAC 2008*.